Impact of Motion on Indirect and Direct Reconstruction of Kinetic Parameters From Dynamic PET Data

Fotis A. Kotasidis, *Member, IEEE* , Charalampos Tsoumpas, *Senior Member, IEEE*, Georgios I. Angelis, *Member, IEEE,* Julian C. Matthews, Andrew J Reader, *Senior Member, IEEE* and Habib Zaidi, *Senior Member, IEEE*

Abstract— **Clinical PET imaging of the abdomen and thorax rely on standardised uptake values using static imaging but more robust quantification can be performed using dynamic protocols and estimating kinetic parameters from the dynamic PET data. However quantitative parameters both in static and dynamic imaging suffer from patient motion. In dynamic imaging the motion-induced data blurring and emission-attenuation mismatch results in erroneous time-activity curves potentially leading to erroneous parametric maps. Furthermore the effects of motion on direct parameter estimates using 4D image reconstruction algorithms are not known. In this work using a novel 5-D numerical body phantom we evaluate the impact of body motion on kinetic parameters in dynamic abdominal and thoracic PET imaging. Furthermore we compared parameter estimates obtained using both conventional post-reconstruction analysis as well as direct 4D image reconstruction.**

***Index Terms*—Direct 4-D image reconstruction, respiratory motion, kinetic modelling**

I. INTRODUCTION

Thoracic and abdominal PET imaging in the clinic typically relies on a static image acquisition for staging newly diagnosed tumours, treatment monitoring or restaging in the event of disease recurrence, with analysis usually restricted to standardised uptake values. Kinetic analysis on the time course of the activity distribution using dynamic image acquisition protocols can provide improved quantification by estimating macro- or micro-parameter maps which directly relate to biologic parameters of interest. However parametric imaging is not routinely using in clinical practice due to its complexity but also due to the fact that dynamic PET data in the body tend to be noisy, resulting in parametric maps of poor precision and accuracy. Direct reconstruction of kinetic parameters can provide parametric maps of improved accuracy and precision in dynamic thoracic and abdominal imaging [1]. However both static and dynamic data suffer from different sources of patient movement occurring during the course of the scan. In the context of static imaging data blurring from motion itself and the mismatch between emission and transmission results in erroneous reconstructed activity concentration images. In the context of dynamic imaging these effects are translated into erroneous time-activity curves (TACs) consequently leading to erroneous voxel-wise parametric maps. In post-reconstruction kinetic analysis such errors are expected to occur at the boundaries of organ structures with diverse kinetics as well as within regions, such as malignant tumours, exhibiting heterogeneous kinetic behaviour. However, analysis so far has been restricted to neuroreceptor imaging studies, where head motion can be considered rigid, and only to macro-parameters [2]. Furthermore the impact of respiratory motion in direct parameter estimates using 4D image reconstruction methods has not be investigated yet.

In this work we use a novel realistic 5-dimensional anthropomorphic phantom to simulate respiratory-induced body motion during a dynamic PET protocol from an $[^{15}O]H_2O$ (single-tissue model) and an $[^{18}F]FDG$ (two-tissue model) scan. Based on this computational phantom we evaluate the impact of respiratory motion both due to data blurring and emission-attenuation mismatch on micro-parameter maps generated using post-reconstruction analysis as well as direct 4D image reconstruction.

II. METHODS

To evaluate the impact of respiratory motion on kinetic parameters from dynamic PET data, a realistic computational 5-D body phantom was developed. The anatomical information, covering the thoracic and upper abdominal area were generated using MRI-derived data to segment the

F.A.Kotasidis is with the Division of Nuclear Medicine & Molecular Imaging, Geneva University Hospital, Geneva, Switzerland and Wolfson Molecular Imaging Centre, MAHSC, University of Manchester, Manchester UK

C. Tsoumpas is with the Department of Biomedical Engineering, Division of Imaging Sciences and Biomedical Engineering, King's College London, St. Thomas' Hospital, London, UK and Division of Medical Physics, University of Leeds, Leeds, UK

J.C. Matthews is with the Wolfson Molecular Imaging Centre, MAHSC, University of Manchester, Manchester UK

G. I.Angelis is with the Brain and Mind Institute, University of Sydney, Sydney, Australia

A.J.Reader is with the Department of Biomedical Engineering, Division of Imaging Sciences and Biomedical Engineering, King's College London, St. Thomas' Hospital, London, UK and Montreal Neurological Institute,McGill University, Montreal, Canada

H. Zaidi is with the Division of Nuclear Medicine and Molecular Imaging, Geneva University Hospital, the Geneva Neuroscience Center, Geneva University, Geneva, Switzerland and the Department of Nuclear Medicine and Molecular Imaging, University of Groningen, University Medical Center Groningen, Groningen, The Netherlands

978-1-4799-0534-8/13/$31.00 ©2013 IEEE

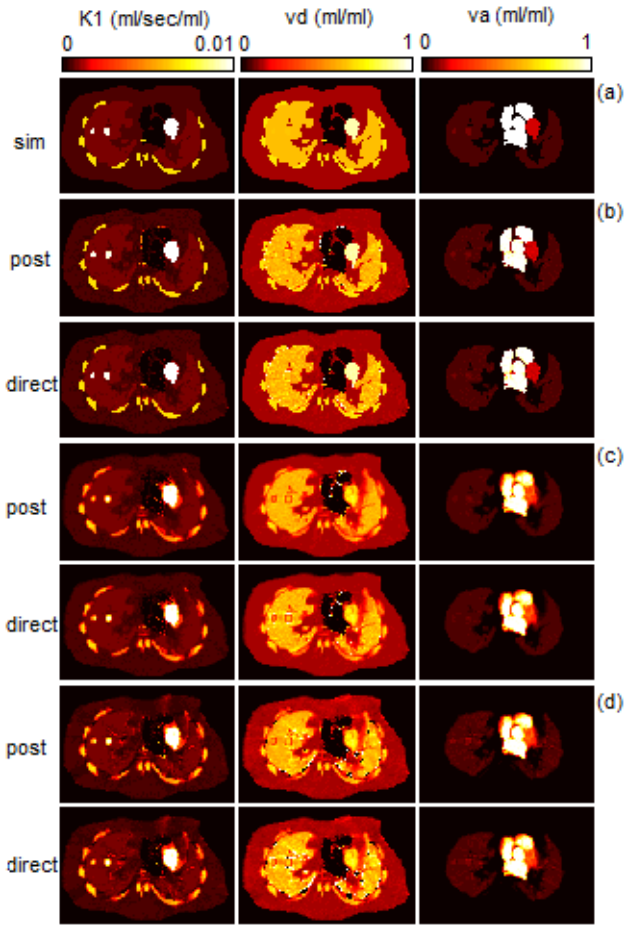

Fig. 1 Simulated parametric images of K_1, vd and bv (a) and reconstructed using the reference gate (no motion) (b), using all gates (data blurring) (c and after introducing attenuation (data blurring + emission-attenuation mismatch) (c) both using direct 4D reconstruction and post-reconstruction analysis of the $[^{15}O]H_2O$ dynamic dataset.

different regions (soft tissue, bones, liver and lungs). The myocardium, heart ventricles and large vessels were segmented using an ECG triggered MRI scan while 9 tumours of different sizes where manually inserted in the liver and lung regions [3-6]. Kinetics typically encountered in dynamic $[^{15}O]H_2O$ and $[^{18}F]$FDG scans were assigned in the MR segmented phantom and TACs were generated using a single-tissue 3 parameter model (K_1, k_2 and blood volume: 28 frames)

$$C_T = IRF(K_1,k_2,t)\otimes C_P + bvC_p = K_1 e^{-k_2 t}\otimes C_p + bvC_p \qquad (1)$$

and a two-tissue 4 parameter model (K_1, k_2, k_3 and blood volume: 29 frames)

$$C_T = IRF(K_1,k_2,k_3,t)\otimes C_P + bvC_p = K_1\left(e^{-(k_2+k_3)t} + \frac{k_3}{(k_3+k_2)}\left(1-e^{-(k_2+k_3)t}\right)\right)\otimes C_p + bvC_p \qquad (2)$$

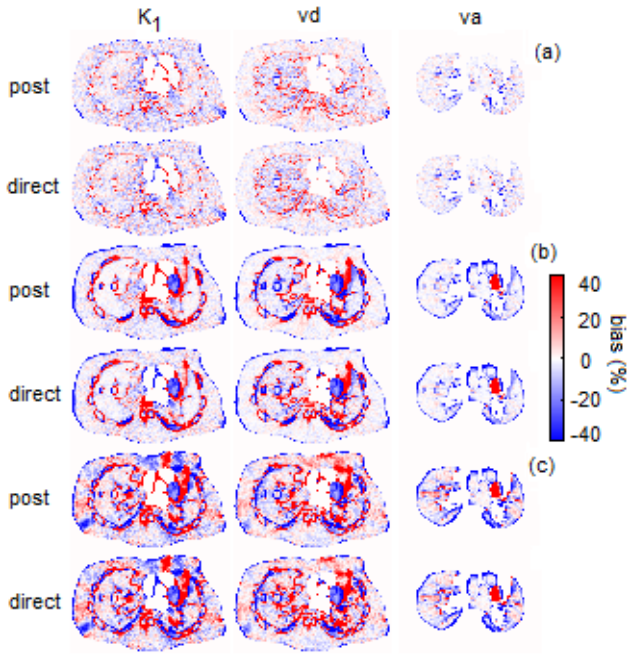

Fig. 2 Bias parametric images of K_1, vd and bv reconstructed using the reference gate (no motion) (a), after using all gates (data blurring) (b) and after introducing attenuation (data blurring + emission-attenuation mismatch) (c) both using direct 4D reconstruction and post-reconstruction analysis of the $[^{15}O]H_2O$ dynamic dataset.

respectively. To simulate motion, motion fields derived from 4D MR images providing a uniform temporal sampling of a complete respiratory cycle, were used to warp the simulated PET data and generate 8 gates for each time frame in the dynamic image sequence [7]. Similar procedure was followed to generate the attenuation maps (air, soft tissue, lungs and bone). The simulated gated emission and attenuation maps were forwarded projected into a virtual scanner using the geometry of the HiRez PET/CT to generate the projection data. Two datasets, with and without attenuation, were generated to decouple the effects on motion and evaluate them separately and in combination. Noiseless datasets were generated initially to evaluate the impact of motion without noise masking any effects. All datasets were reconstructed with 3D reconstruction followed by kinetic analysis, as well as with direct 4D reconstruction [1, 8]. The kinetic models used for parameter estimation matched the ones used to simulate the data (Equations (1) and (2)) and were linearized using the generalized linear least square (GLLS) method to generate the parametric maps [9].

III. RESULTS

Fig. 1 shows the K_1, vd and blood volume parametric images from the dynamic $[^{15}O]H_2O$ noiseless data estimated using the post-reconstruction as well as 4D reconstruction methods. When no motion is simulated (b) both the parameter estimation methods give similar maps and close to the simulated ones (a), with boundaries between regions with

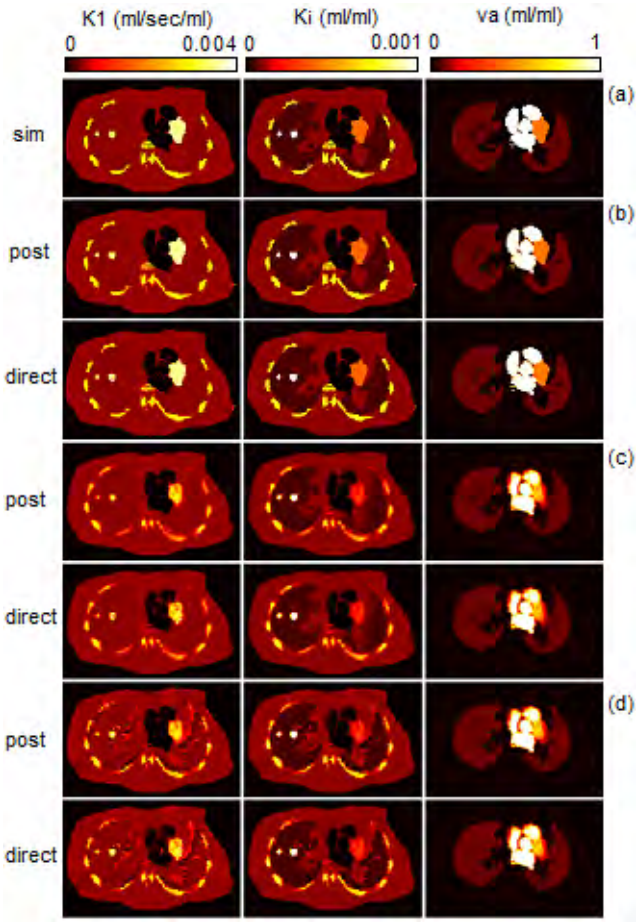

Fig. 3 Simulated parametric images of K_1, K_i and bv (a) and reconstructed using the reference gate (no motion) (b), using all gates (data blurring) (c and after introducing attenuation (data blurring + emission-attenuation mismatch) (c) both using direct 4D reconstruction and post-reconstruction analysis of the [^{18}F]FDG dynamic dataset.

different kinetics, well delineated. When motion was taken into account, parametric maps appear to be blurred with erroneous kinetics at the boundaries of regions with sharp transition in the kinetics. However both the direct and the post-reconstruction methods appear to behave similarly. Further deterioration in the parametric maps is obtained when introducing the emission-attenuation mismatch in the simulation however again both parameter estimation method behave similarly. To better evaluate the different effects of motion, bias parametric maps corresponding to Fig.1 are shown in Fig. 2. Under motionless conditions (a) bias in all regions and parameters is kept under ~3% and due to lack of convergence (10th iteration). Both methods give identical results which is to be expected under noiseless conditions. When motion-induced data blurring was taken into account increased positive and negative bias is observed at the boundaries of structures with the ribs (K_1:-23%, vd:-20%), tumors (K_1:-17%, vd:-5.3%, va:-13%) and myocardium (K_1:-36%, vd:-34%, va:+91%) exhibiting the highest mean bias, with similar results between the 2 parameter estimation

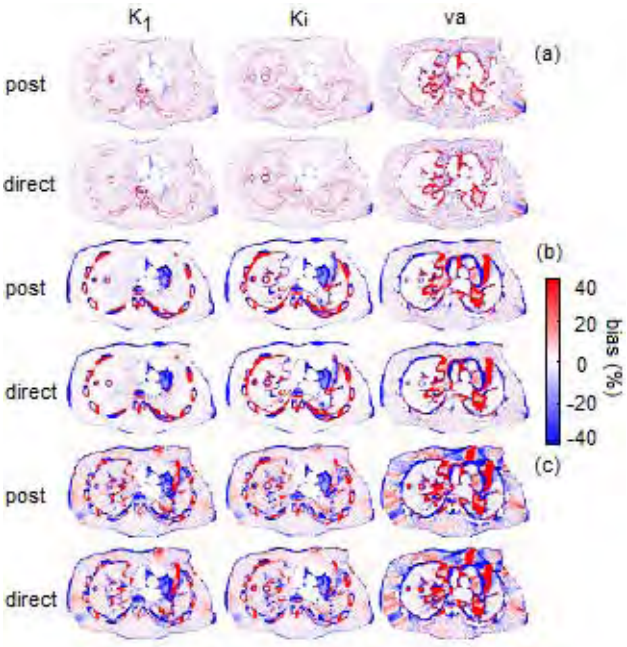

Fig. 4 Bias parametric images of K_1, K_i and bv reconstructed using the reference gate (no motion) (a), after using all gates (data blurring) (b) and after introducing attenuation (data blurring + emission-attenuation mismatch) (c) both using direct 4D reconstruction and post-reconstruction analysis of the [^{18}F]FDG dynamic dataset.

methods. The myocardium wall is of particular interest as being close to the ventricles and aorta is heavily contaminated with the mean blood volume being ~90% positively biased. Including the emission-attenuation mismatch results in substantial voxel-wise positive and negative bias within different regions in both parameter estimation methods, however regional bias is only slightly deteriorated. Similar behaviour is seen in the dynamic [^{18}F]FDG datasets however the blood volume components appears to be slightly more affected compared to K_1 and K_i.

IV. DISCUSSION - CONCLUSION

Respiratory motion-induced data blurring was found to affect kinetic parameters especially at the boundaries of regions. The emission-attenuation mismatch resulted in bias appearing also within regions while at the same time accentuating bias the boundaries of regions with heterogeneous kinetics. No significant difference in bias was found between the 2 parameter estimation methods with the direct 4D reconstruction behaving similar to the post-reconstruction kinetic analysis. It also appears qualitatively that both micro- and macro-parameters are susceptible to motion to a similar degree. Further work is under way to evaluate the effect of motion under noisy conditions.

ACKNOWLEDGMENT

This work was supported by the Swiss National Science Foundation under grant SNSF 31003A-135176 and the EU COST Action TD1007 . C Tsoumpas acknowledges financial contribution of the SUBLIMA EU FP7 grant.

V. REFERENCES

[1] F. A. Kotasidis, A. J. Reader, G. I. Angelis, P. J. Markiewicz, M. D. Walker, P. M. Price*, et al.*, "Direct parametric estimation of blood flow in abdominal PET/CT within an EM reconstruction framework," in *Nuclear Science Symposium Conference Record (NSS/MIC), 2010 IEEE*, 2010, pp. 2868-2874.

[2] H. Herzog, L. Tellmann, R. Fulton, I. Stangier, E. Rota Kops, K. Bente*, et al.*, "Motion artifact reduction on parametric PET images of neuroreceptor binding.," *J Nucl Med,* vol. 46, pp. 1059-1065, Jun 2005.

[3] C. Tsoumpas, C. Buerger, A. P. King, P. Mollet, V. Keereman, S. Vandenberghe*, et al.*, "Fast generation of 4D PET-MR data from real dynamic MR acquisitions.," *Phys Med Biol,* vol. 56, pp. 6597–6613, 2011.

[4] C. Tsoumpas, I. Polycarpou, K. Thielemans, C. Buerger, A. P. King, T. Schaeffter*, et al.*, "The effect of regularization in motion compensated PET image reconstruction: a realistic numerical 4D simulation study," *Phys Med Biol,* vol. 58, pp. 1759-73, Mar 21 2013.

[5] A. P. King, C. Buerger, C. Tsoumpas, P. K. Marsden, and T. Schaeffter, "Thoracic respiratory motion estimation from MRI using a statistical model and a 2-D image navigator," *Med Image Anal,* vol. 16, pp. 252-64, Jan 2012.

[6] C. Buerger, C. Tsoumpas, A. Aitken, A. P. King, P. Schleyer, V. Schulz*, et al.*, "Investigation of MR-Based Attenuation Correction and Motion Compensation for Hybrid PET/MR," *Nuclear Science, IEEE Transactions on,* vol. 59, pp. 1967-1976, 2012.

[7] C. Tsoumpas, J. E. Mackewn, P. Halsted, A. P. King, C. Buerger, J. J. Totman*, et al.*, "Simultaneous PET-MR acquisition and MR-derived motion fields for correction of non-rigid motion in PET.," *Ann Nucl Med,* vol. 24, pp. 745-750, Sep 15 2010.

[8] J. C. Matthews, G. I. Angelis, F. A. Kotasidis, P. J. Markiewicz, and A. J. Reader, "Direct reconstruction of parametric images using any spatiotemporal 4D image based model and maximum likelihood expectation maximisation," in *Nuclear Science Symposium Conference Record (NSS/MIC), 2010 IEEE*, 2010, pp. 2435-2441.

[9] F. Dagan, S. C. Huang, W. ZhiZhong, and H. Dino, "An unbiased parametric imaging algorithm for nonuniformly sampled biomedical system parameter estimation," *Medical Imaging, IEEE Transactions on,* vol. 15, pp. 512-518, 1996.